AGU PUBLICATIONS

JGR

Journal of Geophysical Research: Space Physics

RESEARCH ARTICLE

10.1002/2014JA020669

Key Points:
- Thermal effects on 1–10 kHz whistler mode waves are calculated for the first time
- Ion temperature is more significant than electron temperature
- Use of in situ sources needs to be reassessed

Correspondence to:
M. Gołkowski,
mark.golkowski@ucdenver.edu

Citation:
Kulkarni, P., M. Gołkowski, U. S. Inan, and T. F. Bell (2015), The effect of electron and ion temperature on the refractive index surface of 1–10 kHz whistler mode waves in the inner magnetosphere, *J. Geophys. Res. Space Physics*, *120*, 581–591, doi:10.1002/2014JA020669.

Received 2 OCT 2014
Accepted 29 DEC 2014
Accepted article online 7 JAN 2015
Published online 30 JAN 2015

The effect of electron and ion temperature on the refractive index surface of 1–10 kHz whistler mode waves in the inner magnetosphere

P. Kulkarni[1], M. Gołkowski[2], U. S. Inan[3,4], and T. F. Bell[4]

[1]Intapp, Palo Alto, California, USA, [2]Department of Electrical Engineering, University of Colorado Denver, Denver, Colorado, USA, [3]Department of Electrical Engineering, Koc University, Istanbul, Turkey, [4]Department of Electrical Engineering, Stanford University, Stanford, California, USA,

Abstract Whistler mode waves in the magnetosphere play an important role in the energy dynamics of the Earth's radiation belts. Previous theoretical work has been extended to include ions in the fully adiabatic warm plasma theory. Using a finite electron and ion temperature of 1 eV, refractive index surfaces are calculated for 1–10 kHz whistler mode waves in the inner magnetosphere ($L \lesssim 2.5$). For the frequencies of interest, a finite ion temperature is found to have a greater effect on the refractive index surface than the electron temperature and the primary effect is to close an otherwise open refractive index surface. Including a finite ion temperature is especially important when the wave frequency is just above the local lower hybrid resonance frequency. For wave frequencies more than ~1 kHz above the local lower hybrid resonance frequency, including the ion temperature has a negligible effect on the refractive index surface calculation. The results are used to assess previous conclusions on whether in situ whistler mode sources can be realistically used to precipitate energetic electrons. It is found that the number of in situ sources needed to illuminate the inner plasmasphere ($L \lesssim 2.5$) with whistler mode energy may be greater than previously predicted.

1. Introduction

Resonant interactions between very low frequency (VLF) waves and energetic electrons are a primary loss mechanism for energetic particles trapped in the Earth's radiation belts [*Kennel and Petschek*, 1966; *Lyons et al.*, 1972; *Inan*, 1987]. The landmark study by *Abel and Thorne* [1998a, 1998b] estimated loss rates of energetic radiation belt electrons in the 100–1500 keV energy range induced by resonant interactions with a variety of plasma waves, including plasmaspheric hiss, lightning-generated whistlers, and VLF transmitter signals. It was found that anthropogenic, ground-based VLF sources have a significant impact on 100–1500 keV electron lifetimes at $L \lesssim 2.6$. The actual amplitudes of ground-based anthropogenic VLF sources in the magnetosphere have recently been a topic of active discussion in the literature [*Starks et al.*, 2008; *Tao et al.*, 2010; *Foust et al.*, 2010; *Shao et al.*, 2012; *Graf et al.*, 2013]. Overall, there is a consensus that man-made sources play a measurable role in radiation belt dynamics and this has been the motivation behind several dedicated wave injection experiments with ground-based VLF sources [*Inan et al.*, 2007; *Graf et al.*, 2011; *Gołkowski et al.*, 2011].

Inan et al. [2003] proposed the use of spacecraft to radiate whistler mode waves directly into the inner radiation belts for controlled precipitation of energetic electrons. In situ injection eliminates the problem of ionospheric absorption that limits the effectiveness of ground-based injection. Comparison to the results of *Abel and Thorne* [1998a, 1998b], led *Inan et al.* [2003] to conclude that a spaceborne transmitter has the potential to drive diffusion rates an order of magnitude greater than that of ground-based VLF transmitters in the key band of 1–10 kHz. Another advantage of in situ injection is the opportunity to more easily leverage magnetospheric reflections [*Edgar*, 1972], which allows a single wave packet to continually propagate in the magnetosphere for several seconds. Magnetospheric reflections do not occur for wave frequencies of 16–50 kHz that are more typical of stationary ground-based transmitters.

Although the study by *Inan et al.* [2003] made a strong case for the effectiveness of deploying in situ sources for precipitation of radiation belt electrons, three key issues on the feasibility of such an approach were left unanswered. First, it was necessary to investigate how whistler mode wave energy from an in situ source would be dispersed throughout the inner magnetosphere. If, for example, raypaths do not propagate far

Table 1. The Wave Frequencies Simulated for the Six Different Injection Sites Considered Here[a]

	Local Lower Hybrid Resonance Frequency			
	$\lambda_s = 0°$		$\lambda_s = 20°$	
	5.4 kHz		9 kHz	−89.3°
$L = 1.5$	6 kHz	−89.3°	10 kHz	−89°
	7 kHz	−88.9°	11 kHz	−88.8
	2.3 kHz		3.8 kHz	
$L = 2.0$	2.5 kHz	−89.9°	4.2 kHz	−89.6°
	3.5 kHz	−88.7°	5.2 kHz	−88.9°
	1.2 kHz		2.0 kHz	
$L = 2.5$	1.3 kHz		2.2 kHz	−89.8°
	2.3 kHz	−88.1°	3.2 kHz	−88.5°

[a]At each location, the middle frequency is approximately equal to the local f_{LHR} while the top and bottom frequencies are ~10% below and 1 kHz above, respectively. Also shown re the resonance cone angles whenever they exist (i.e., whenever the frequency considered is above the local f_{LHR}).

from the source, filling the plasmasphere with VLF wave energy may require numerous transmitters. Second, the energetic electron precipitation induced by such sources would have to be calculated. Even if the inner plasmasphere could be filled with VLF wave energy, such sources would be ineffective in a scheme of controlled precipitation if they did not sufficiently precipitate energetic electrons. Finally, and in connection with the second issue, *Inan et al.* [2003] noted that waves with frequencies of several kilohertz exiting a source would propagate with a wave normal angle, ψ very close to the resonance cone, ψ_{res}. The diffusion estimates presented in *Inan et al.* [2003], however, were for waves at constant $\psi = 45°$. It was therefore crucial to carefully treat the effect of ψ on electron precipitation.

The first issue mentioned above was addressed by *Kulkarni et al.* [2006], while *Kulkarni et al.* [2008] addressed the second and third. Specifically, the former study used numerical ray tracing, a Landau damping calculation and a realistic model of antenna propagation in a magnetoplasma to conclude that three transmitter sources at $L = 1.5$, $L = 2$, and $L = 2.5$ can effectively fill the plasmaspheric cavity with VLF wave energy. The latter study calculated precipitation signatures and investigated the effect of waves that propagate with ψ very close to ψ_{res}. The authors concluded that, despite the issues raised by *Inan et al.* [2003], magnetospherically reflecting whistler mode waves from an in situ source can be used to effectively target 1 MeV–5 MeV electrons.

The ray tracing calculations performed by *Kulkarni et al.* [2006, 2008] neglected the effects of finite ion and electron temperature in determining wave propagation trajectories in a cold, smooth magnetosphere. However, a finite electron and/or ion temperature can affect the propagation of wave energy, which in turn might modify the calculated precipitation signatures. Here we include finite particle temperature and investigate how this affects the conclusions of *Kulkarni et al.* [2006] and *Kulkarni et al.* [2008] that we hereafter refer to as Paper I and Paper II, respectively. To do so, we extend previous work [*Sitenko and Stepanov*, 1957; *Buneman*, 1961; *Aubry et al.*, 1970] to include the effects of positive ions in a fully adiabatic warm plasma theory and calculate relevant refractive index surfaces.

All of the results in this work are based on a dipole model of the geomagnetic field and cold plasma density according to *Carpenter and Anderson* [1992] under geomagnetically quiet conditions, with plasmapause at $L = 5.5$. In addition to electrons, the plasma contains three species of ions: hydrogen, helium, and oxygen. (The effect of the various plasma constituents are also examined below.) For reference, Table 1 shows the in situ locations and frequencies that were used in Papers I and II, and are used here. As in the previous related work, we select initial wave normal angles that are no farther than 3° from the local resonance cone. The frequency values are bounded from above because wave frequencies much higher than the local f_{LHR} would be Landau damped too quickly (1–2 s) to induce appreciable precipitation. The frequency is bounded from below because, as implied by the *Wang and Bell* [1969] model of antenna radiation in a magnetoplasma, there is negligible radiated power for waves more than 10% below the local f_{LHR}. A similar rationale explains the wave normal angle range chosen. See the Appendix in Paper II for a more complete description.

2. Theoretical Background

As mentioned above, including a finite temperature in our calculations may modify the precipitation signatures shown in Paper II by changing the propagation characteristics of the injected wave packets. Specifically, the magnetospheric reflection point may move to lower geomagnetic latitudes, and the wave

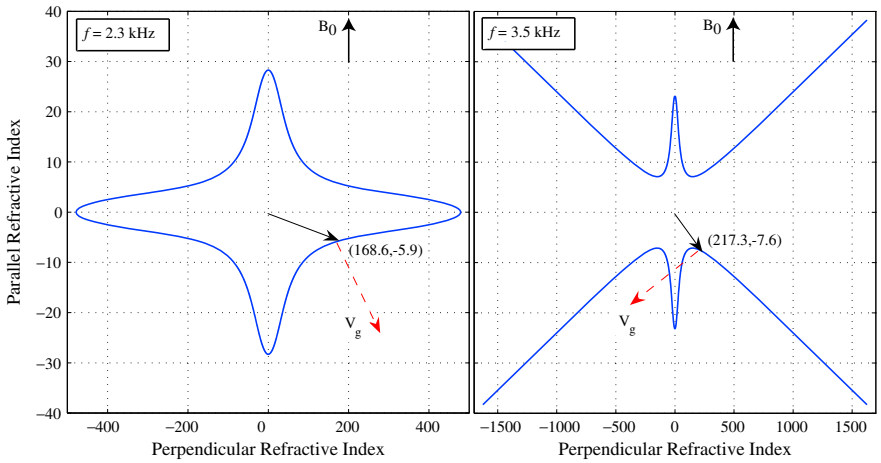

Figure 1. (a) Refractive index surface for a 2.3 kHz wave at the equator at $L = 2$ (f_{LHR} ~2.47 kHz). The arrow in black is the refractive index vector μ at a wave normal angle of −88°. The coordinates in parentheses are the value of μ at that location. The dashed arrow in red shows the direction of the wave group velocity at that point. (b) Similar to Figure 1a but for 3.5 kHz waves. Note that the magnitude of μ at $\psi = -85°$ is larger than that in Figure 1a, and that the refractive index surface is open rather than closed. Magnetospheric reflections cannot occur under this situation.

k vector direction may be farther from the resonance cone angle. Completely determining how thermal effects will change the results shown in Paper II would require incorporating a finite ion temperature in numerical ray tracing. In the absence of a fully developed warm plasma ray tracing program, we can still make indirect, quantitative estimates of the effect of temperature by calculating its effect on the refractive index μ. In the ray tracing often used in space physics, pioneered by *Haselgrove* [1954], which includes the Stanford VLF ray tracing program [*Inan and Bell*, 1977], the refractive index is used to capture all key properties of the propagation medium. For a fixed frequency at a given location in the magnetosphere, the plasma density and various gyrofrequencies are constant, and the refractive index is often displayed as a polar plot of μ versus the wave normal angle, ψ, where the polar axis is parallel to the ambient magnetic field B_0. These so-called refractive index surfaces, $\mu(\psi)$, are useful in studying whistler mode ray propagation because the wave group velocity for a specified ψ is normal to the surface [*Helliwell*, 1965, p. 34; *Poeverlein*, 1948].

Figures 1a and 1b show sample refractive index surfaces at the equator at $L = 2$, without inclusion of thermal effects. We have selected wave frequencies of 2.3 kHz and 3.5 kHz to correspond to the frequencies used in Papers I and II. We have specified the perpendicular and parallel (with respect to the ambient magnetic field, B_0) value of μ and the direction of the group velocity, V_g, at $\psi = 88°$ for both frequencies. Note that $\mu(\psi)$ for 2.3 kHz describes a closed surface, while the surface is open for 3.5 kHz. Magnetospheric reflections can occur only at points at which the refractive index surface is closed. Warm plasma theory indicates that a finite temperature closes the refractive index surface at frequencies that would exhibit open refractive index surfaces in the absence of thermal effects. That is, thermal effects would close the refractive index surface for 3.5 kHz waves, the opposite of the cold plasma surface shown in Figure 1b. It is this change—closing $\mu(\psi)$ earlier along a given raypath—that results in magnetospheric reflection occurring at a lower latitude, and thereby possibly changing the results shown in Paper II.

We now describe the methodology used to calculate the refractive index surfaces, emphasize the role of a finite ion versus electron temperature at the frequencies considered here, and elaborate on why the f_{LHR} represents a crossover frequency for the purpose of this study.

2.1. Fully Adiabatic Warm Plasma Theory

If a plasma is modeled as a fluid by taking appropriate moments of the Boltzmann equation and velocity space distribution function, temperature is accounted for by adding a pressure term to the momentum transport equation. Standard plasma physics textbooks often assume a scalar pressure and either an adiabatic or isothermal equation of state to close the infinite set of moment equations [*Bittencourt*, 2004, chapter 17]. While this approach is useful from a pedagogical standpoint, these assumptions often do not yield sufficient accuracy as compared to the results from kinetic theory [*Fang and Andrews*, 1971]. Instead

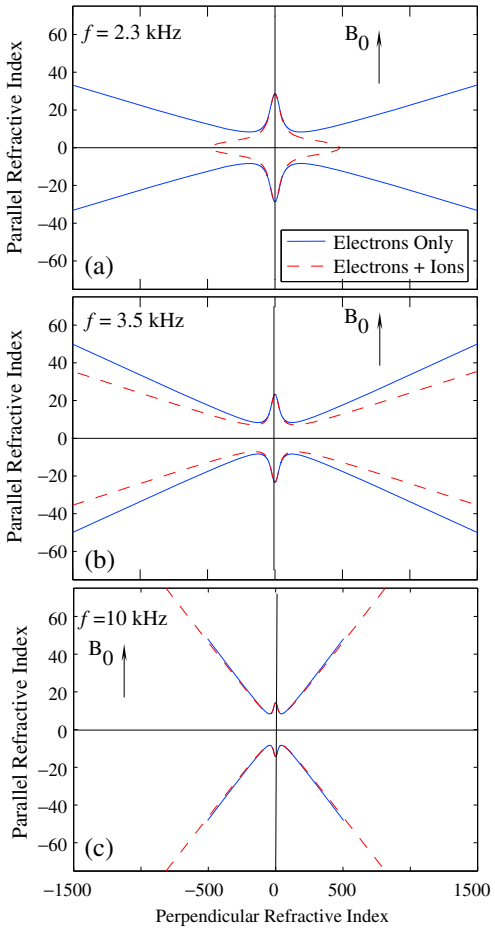

Figure 2. Refractive index surfaces for (a) 2.3, (b) 3.5, and (c) 10 kHz waves at $L = 2$ at the equator. Note that ions are needed to close the surface for 2.3 kHz waves (below the local f_{LHR} ~2.47 kHz), and the surface remains open even with the inclusion of ions for 3.5 and 10 kHz waves.

of a scalar pressure combined with an equation of state, many authors have therefore used a so-called fully adiabatic warm plasma theory where temperature corrections are added to all terms of the kinetic pressure tensor, not only the diagonal elements [*Sitenko and Stepanov*, 1957; *Buneman*, 1961; *Aubry et al.*, 1970; *Fang and Andrews*, 1971]. This approach essentially neglects the divergence of the heat flux in the development of the moment equations.

The fully adiabatic warm plasma theory results in a sixth-order equation for the refractive index, as opposed to the fourth-order equation that follows the cold plasma assumption. Using a notation and development similar to that of previous works, we can write the warm plasma dispersion relation as follows:

$$q^{\mathrm{T}}A_1\mu^6 + (A_0 + q^{\mathrm{T}}B_1)\mu^4 + (B_0 + q^{\mathrm{T}}C_1)\mu^2 + C_0 = 0 \quad (1)$$

where the coefficients A_0, B_0, A_1, etc. are related to components of the cold and warm plasma dieletric tensors (described below). Subscripts "0" refer to cold plasma parameters and subscripts "1" refer to warm plasma parameters. The parameter $q^{\mathrm{T}} = k_B T_j / m_j c^2$ accounts for the effect of temperature, where k_B is Boltzmann's constant, T_j and m_j are respectively the temperature in Kelvin and mass of the jth plasma species, and c is the speed of light [*Sitenko and Stepanov*, 1957; *Aubry et al.*, 1970; *Fang and Andrews*, 1971]. A_0, B_0, and C_0 are defined by the cold plasma dielectric tensor, K^0:

$$K^0 = \begin{bmatrix} 1 - \sum_j \frac{X}{1-Y^2} & \sum_j \frac{iXY}{1-Y^2} & 0 \\ \sum_j \frac{-iXY}{1-Y^2} & 1 - \sum_j \frac{X}{1-Y^2} & 0 \\ 0 & 0 & 1 - X \end{bmatrix} \quad (2)$$

where $X = \omega_{pj}^2/\omega^2$, $Y = \omega_{cj}/\omega$, $\omega_{pj} = q_j^2 N_j/\epsilon_0 m_j$, and $\omega_{cj} = q_j \mathbf{B_0}/m_j$ are respectively the plasma and cyclotron frequency of the jth plasma species, q_j, N_j, and m_j are the corresponding charge, density, and mass, B_0 is the magnitude of the ambient magnetic field, ϵ_0 is the permittivity of free space, ω is the angular wave frequency, and $i = \sqrt{-1}$. The summation is over the four plasma species (electron, hydrogen, helium, and oxygen ions). Referencing the components of K^0 above allows us to define A_0, B_0, and C_0, simply the coefficients of the cold plasma dispersion relation, in equation (1):

$$A_0 = K_{11}^0 \sin^2\psi + K_{33}^0 \cos^2\psi$$
$$B_0 = -[K_{11}^0 K_{22}^0 + K_{12}^0]\sin^2\psi - K_{33}^0[K_{11}^0 + K_{22}^0\cos^2\psi]$$
$$C_0 = K_{33}^0[(K_{12}^0)^2 + K_{11}^0 K_{22}^0]$$

Note that in cold plasma theory, the coefficients A_1, B_1, and C_1 are all zero.

We can add a linear temperature correction to K^0 above: $K = K^0 + \tau K^1$, where K is the total dielectric tensor, K^1 is the warm plasma correction, and $\tau = q^T \mu^2$. The components of K^1 are given in *Aubry et al.* [1970]

$$K_{11}^1 = \sum_j \left[\frac{-X}{1-Y^2} \left(\frac{3\sin^2\psi}{1-4Y^2} + \frac{1+3Y^2}{(1-Y^2)^2}\cos^2\psi \right) \right] \tag{3}$$

$$K_{22}^1 = \sum_j \left[\frac{-X}{1-Y^2} \left(\frac{1+8Y^2}{1-4Y^2}\sin^2\psi + \frac{1+3Y^2}{(1-Y^2)^2}\cos^2\psi \right) \right] \tag{4}$$

$$K_{33}^1 = \sum_j \left[-X \left(3\cos^2\psi + \frac{\sin^2\psi}{1-Y^2} \right) \right] \tag{5}$$

$$K_{12}^1 = -K_{21}^2 = \sum_j \left[i\frac{X}{1-Y^2} \left(\frac{6\sin^2\psi}{1-4Y^2} + \frac{3+Y^2}{(1-Y^2)^2}\cos^2\psi \right) \right] \tag{6}$$

$$K_{23}^1 = -K_{32}^2 = \sum_j \left[-i\frac{XY}{(1-Y^2)^2}(3-Y^2)\sin\psi cos\psi \right] \tag{7}$$

$$K_{13}^1 = K_{31}^2 = \sum_j \left[\frac{2X}{(1-Y^2)^2}\sin\psi cos\psi \right] \tag{8}$$

where X, Y, and ψ have been defined above. We have added a summation over all the plasma species, whereas previous authors included only electrons in their calculations. We can now define A_1, B_1, and C_1 as a function of the components of K^1 and K^0:

$$A_1 = K_{11}^1 \sin^2\psi + K_{33}^1 \cos^2\psi + 2K_{13}^1 \sin\psi\cos\psi \tag{9}$$

$$B_1 = -[K_{11}^1 K_{22}^0 + K_{22}^1 K_{11}^0 + 2K_{12}^0 K_{12}^1]\sin^2\psi - K_{33}^1[K_{11}^0 + K_{22}^0\cos^2\psi] - K_{33}^0[K_{11}^0 + K_{22}^0\cos^2\psi] + 2\sin\psi\cos\psi[K_{12}^0 K_{23}^1 - K_{13}^1 K_{22}^0] \tag{10}$$

$$C_1 = K_{33}^1[(K_{12}^0)^2 + K_{11}^0 K_{22}^0] + K_{33}^0[2K_{12}^0 K_{12}^1 + K_{11}^0 K_{22}^1 + K_{11}^1 K_{22}^0] \tag{11}$$

We use the above equations to calculate refractive index surfaces at a number of locations, operating frequencies, and plasma temperatures. As described above, we specifically investigate 1–10 kHz magnetospherically reflecting whistler mode waves. Previous authors who used the fully adiabatic warm plasma theory studied frequencies close to the upper hybrid resonance frequency and the electron plasma frequency, which are not relevant to in situ injection and propagation of whistler mode waves in the inner magnetosphere ($L < 2.5$) [*Aubry et al.*, 1970; *Fang and Andrews*, 1971]. A series of papers [*Sazhin*, 1985; *Sazhin and Sazhina*, 1985; *Sazhin*, 1986] presented approximate analytical formulas for wave propagation in hot anisotropic plasmas, but only considered finite electron temperatures, and were also restricted to frequencies above the gyrofrequency. *Hashimoto et al.* [1977] did study the temperature effects on VLF wave propagation, but modeled wave frequencies much larger than f_{LHR}, where ions are relatively unimportant [see below; *Kimura*, 1966; *Mann et al.*, 1997]. To the best of our knowledge, no previous work using the fully adiabatic warm plasma theory analyzed the effects of finite ion temperature. In the conclusion we address limitations of the fully adiabatic warm plasma theory and possible modifications to our results if the more exact kinetic theory is used. We now emphasize the importance of ions, and therefore a finite ion temperature, and the f_{LHR} at the frequencies considered in this study.

2.2. Importance of Ions and the Lower Hybrid Resonance Frequency (f_{LHR})

Hines [1957] and *Kimura* [1966] were the first to consider the effects that ionic species would have on whistler mode propagation in the magnetosphere. The latter work incorporated three species of ions (hydrogen, helium, and oxygen), and demonstrated that their inclusion is essential to closing the refractive index surface. The necessity of ion presence to close the refractive index surface is illustrated in Figure 2, which shows plots of $\mu(\psi)$ for 2.3, 3.5, and 10 kHz waves at the equator at $L = 2$, still without inclusion of thermal effects. For each frequency, we have shown the effect of including only electrons and electrons as well as ions. When ions are neglected, $\mu(\psi)$ is open for all frequencies. Because $\mu(\psi)$ must be closed for magnetospheric reflections to occur, we lose essential physics if ions are ignored in the ray tracing formulation. Note, however, that if $f > f_{LHR}$ (as in Figures 2b and 2c), ions do not change the topology of the refractive index surface. In fact, for a wave frequency of 10 kHz, $\mu(\psi)$ shows a negligible difference whether ions are included or not. Including ions in the numerical ray tracing and $\mu(\psi)$ calculation is therefore critical

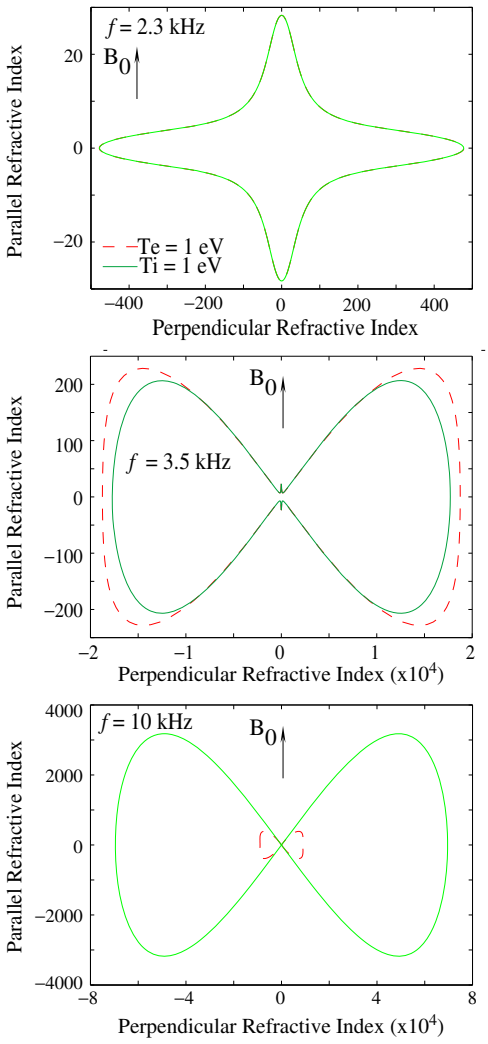

Figure 3. (top, middle, and bottom) Refractive index surfaces for the same wave frequencies as Figure 2. Note that including an ion temperature of 1 eV closes the surface more quickly than an electron temperature of 1 eV for 3.5 kHz waves. Contrast Figure 2 (middle) here with Figure 2b, where the refractive index surface is open.

at frequencies below and just above the f_{LHR}. A few kilohertz above the f_{LHR}, ions are relatively unimportant [*Kimura*, 1966].

We now investigate the effect that inclusion of a finite ion or electron temperature has on the refractive index surface. To do so, we use equation (1) to calculate $\mu(\psi)$ at a similar location and for similar frequencies as shown in Figure 2. We have included three ionic species plus electrons in our calculations but assigned a finite temperature of 1 eV only to electrons and hydrogen ions. As discussed in more detail below, helium and oxygen ions have a negligible effect for the freqeuncies of interest. Figure 3 displays refractive index surfaces calculated with finite temperatures. Observe first that for 2.3 kHz waves, there is no change to $\mu(\psi)$ whether T_e=1 eV, or T_i = 1 eV—a result that is true for any frequency below the local f_{LHR}. This point is crucial to our analysis below, and we therefore reiterate: for $f < f_{LHR}$, a finite electron or ion temperature has no effect on $\mu(\psi)$ (compare Figures 2a and 3, top).

For 3.5 kHz waves at the equator at $L = 2$, Figure 3 shows that, compared to Figure 2b, $\mu(\psi)$ closes when temperature is included. There are two additional noteworthy features of this panel. First of all, T_i=1 eV closes $\mu(\psi)$ more tightly than does $T_e = 1$ eV. That is, for corresponding wave normal angles, the magnitude of μ is smaller for a finite ion temperature than for a finite electron temperature. Primarily because of this result—which holds for frequencies slightly above the local f_{LHR}—we conclude that at the frequencies of interest, a finite ion rather than electron temperature will more strongly affect wave propagation. Second, the magnitude of μ close to the resonance cone is not appreciably different from the case where $T_i = 0$. So while a finite ion temperature does close $\mu(\psi)$, which would be open with T_i=0, at ψ close to ψ_{res}, the difference appears to be marginal. Figure 3 (bottom) shows that, unlike for 3.5 kHz waves, 10 kHz waves at L=2 are more affected by T_e instead of T_i. This result is consistent with our analysis above—the effects of ions become relatively less important at frequencies several kilohertz above the local f_{LHR}.

We now consider the case when the wave frequency is approximately equal to (within 500 Hz of) the local f_{LHR}. In this case a finite T_i can dramatically change the refractive index surface. Consider Figure 4, which shows $\mu(\psi)$ for 2.3, 2.45, and 2.5 kHz waves at the equator at $L = 2$, where the local f_{LHR} is 2.47 kHz. We have plotted the refractive index surface with both $T_i = 0$ and $T_i = 1$ eV. We have ignored T_e because, as discussed above, T_i is more important at these frequencies. In Figures 4a and 4b (both below f_{LHR}), $\mu(\psi)$ is closed and basically unchanged whether temperature is included or not. But for a 2.5 kHz wave, Figure 4c shows that $T_i = 1$ eV tightly closes the refractive index surface. For these types of frequencies, where $f \sim f_{LHR}$, including T_i will affect the ray tracing calculation more significantly than when the frequency is less than or more than ~1 kHz above the local f_{LHR}.

Before proceeding, we briefly review the main points of our analysis. Ultimately, we are interested in accessing the efficacy of in situ sources in precipitating > 1 MeV electrons from the inner radiation belts

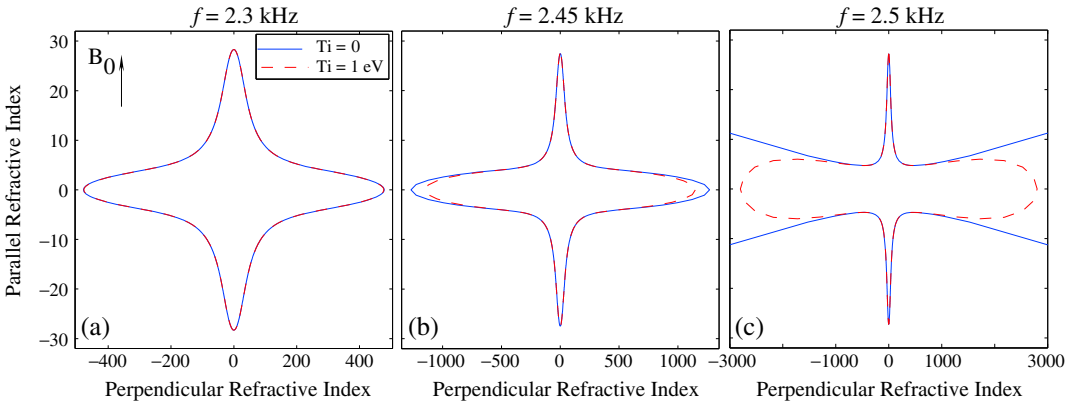

Figure 4. (a–c) Refractive index surfaces for waves at the equator at $L = 2$. Waves below the local f_{LHR} ~2.47 kHz are not strongly affected by a finite ion temperature. For 2.5 kHz waves, however, including $T_i = 1$ eV dramatically closes an otherwise open cold plasma refractive index surface.

($L \lesssim 2.5$). These issues have been investigated in Papers I and II; we now include finite particle temperatures because the assumption of a cold magnetoplasma is not always valid. Specifically, if a finite electron or ion temperature is included in the ray tracing formulation, the raypaths may be different, which would modify the precipitation signatures shown in Paper II. Because the refractive index, μ, is central to the ray tracing calculation, determining how and when μ changes with temperature has been the focus of this study. For the few kilohertz whistler mode waves that would be injected from a source in the inner magnetosphere, the relevant results and conclusions thus far can be summarized as follows:

1. Warm plasma theory may modify the raypath in two main ways: a lower magnetospheric reflection point, and a different k vector along the raypath.
2. A magnetospheric reflection can occur if and only if the refractive index surface, $\mu(\psi)$ is closed.
3. Ions are essential for closing $\mu(\psi)$, which is always open without ions.
4. For frequencies several kilohertz above f_{LHR}, ions are relatively unimportant and the refractive index surface is open if temperature effects are ignored.
5. For frequencies within ~1 kHz of the local f_{LHR}—the frequencies of interest here—T_i is more important than T_e.
6. A finite T_i has the most dramatic effect on $\mu(\psi)$ for wave frequencies that are greater than the local f_{LHR} (e.g., 2.5 kHz at the equator at $L = 2$) by only a few hundred hertz or less. The effect is to close an otherwise open refractive index surface (see Figures 3 and 4).

The above points all refer to the specific frequencies of interest. An empirical survey of the frequency dependence normalized to f_{LHR} revealed that the thermal effects of ions have a significant impact on the refractive index surface for the frequency range $0.97f_{LHR} < f < 1.6f_{LHR}$

Finally, we briefly address the effect of a finite temperature for the remaining ionic species: helium and oxygen. As described by *Mann et al.* [1997], as long as the wave frequency is not much lower than f_{LHR}, the hydrogen ion dominates the other ions in calculating μ. Given that we only consider $f > 0.9f_{LHR}$, these ions do not affect our results. Furthermore, we have calculated $\mu(\psi)$ for hydrogen, helium, and oxygen temperatures of 1 eV (not shown) and confirmed the conclusions presented in *Mann et al.* [1997]. Of the four plasma species discussed, a finite hydrogen ion temperature will most strongly modify the results shown in Papers I and II. A finite electron, helium, or oxygen temperature, on the other hand, would have a negligible effect.

3. Effects on Energetic Electron Precipitation

We now assess the implications of the above results on the issue of in situ whistler mode sources for energetic electron precipitation from the radiation belts. We first restate the major conclusions from Papers I and II. Paper I used numerical ray tracing and a Landau damping calculation to conclude that three transmitter sources at $L = 1.5$, $L = 2$, and $L = 2.5$ can fill the plasmaspheric cavity with VLF wave energy. It should be noted that each transmitter illuminates a region no greater than $0.2L$ from the source L shell.

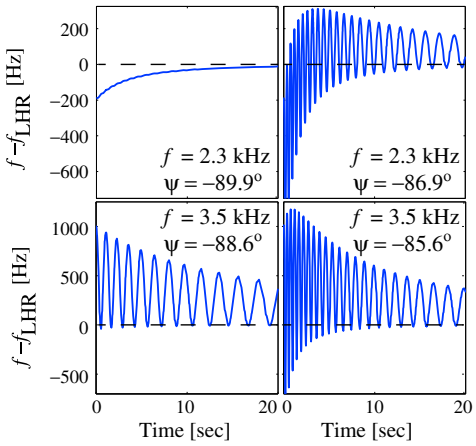

Figure 5. Difference between the wave frequency and the local f_{LHR} for propagating wave packets as a function of time for injections at four different combinations of frequency and wave normal angle. Waves are injected at the equator at $L = 2$ ($f_{LHR} \sim 2.47$ kHz) with wave normal angle Ψ. Ray tracing is performed under the cold plasma assumption.

Paper II presented precipitation signatures that would be induced by those sources, and it was concluded that 1 MeV–5 MeV electrons can be effectively targeted. Even though the waves injected from such sources propagate with wave normal angles very close to the local resonancecone, significant energetic electron precipitation would result.

As shown above, when $f > f_{LHR}$, the cold plasma assumption used in calculating these results no longer holds and a warm plasma refractive index should be used in the ray tracing calculation. Figure 5 shows the difference between the wave frequency and the local f_{LHR}, $f - f_{LHR}$, for 2.3 kHz and 3.5 kHz waves along the ray path as they propagate away from their source at the transmitter. For both frequencies, we have injected rays at two distinct wave normal angles: 2.3 kHz at initial $\psi = -89.9°$ and $-86.9°$, and 3.5 kHz initially at $\psi = -88.6°$ and $-85.6°$. These values correspond to the local ψ_{res} and $\psi_{res} + 3°$ (see Table 1, above and Paper II for the justification of these numbers). Note that, other than a 2.3 kHz ray injected at $\psi = -89.9°$, $f - f_{LHR}$ drops below zero several times along the path, indicating that the refractive index surface is open if thermal effects are neglected. It is at these portions of the raypath that a finite T_i should be incorporated. Our analysis therefore proceeds by determining what portion of these raypaths as calculated by the cold plasma Stanford VLF ray tracing would be modified by thermal effects.

Using these parameters (shown in Figure 5), we trace rays for 20 s (as was done for the results shown in Paper II) and define the ray lifetime as the shorter of 20 s or the time for attenuation by 10 dB. The latter consideration accounts for the differential damping rate for various wave frequencies and initial wave normal angles considered. Because a 3.5 kHz ray injected at −85.6° is fully damped within 15 s (not shown), it would be unreasonable to define its lifetime as 20 s. We then calculate how much time the ray propagates with its wave frequency above the local f_{LHR}. This time is divided by the ray lifetime to yield a percentage of a given raypath that may be affected by a finite T_i. Figure 6 shows the results of this calculation. We can see that according to the metrics just specified, thermal effects should be incorporated for significant portions of these raypaths. Without a fully developed warm plasma ray tracer, however, these results alone do not determine exactly how the raypaths will change. *Hashimoto et al.* [1977], using a similar development as we have, noted that for 22.3 kHz waves (still in the VLF range), warm plasma theory does not significantly change the raypath despite changing μ. The authors noted that incorporating warm plasma theory changed ψ as well as μ, with the end result being an almost identical raypath. However, as discussed above, *Hashimoto et al.* [1977] did not include ions and did not study 1–10 kHz magnetospherically reflecting whistler mode waves. The few raypaths shown in that study made only a single traverse of the magnetosphere. Over several magnetospheric reflections, it is possible that the small modifications over individual segments combine to yield a different distribution of wave energy.

For the parameters chosen, *Kulkarni et al.* [2006, 2008] show that the region of illumination is never more than $0.2L$ from the source site. For example, 2.3 kHz waves injected from $L = 2$ illuminate up to $L = 2.2$, and 3.5 kHz waves illuminate between $L = 1.9$ and $L = 2$. Given that the effect of warm plasma theory would be to close the refractive index surface along the raypath, resulting in an earlier magnetospheric reflection, we estimate that the overall region of illumination will be somewhat reduced. Especially for waves injected at the geomagnetic equator, magnetospheric reflections often occur within 10° of the geomagnetic equator (see Figure 9 and associated discussion in Paper II). So warm plasma theory may nominally change the latitude of the reflection point by 2° from, say, $\lambda = 10°$ to $\lambda = 8°$. Instead of projecting whistler mode wave energy as far as $L = 2.2$ with an equatorial source at $L = 2$, such waves may only traverse up to $L = 2.1$. However, damping effects due to finite temperatures would also need to be investigated. Off-equatorial injections, however, propagate to higher geomagnetic latitudes, and thermal

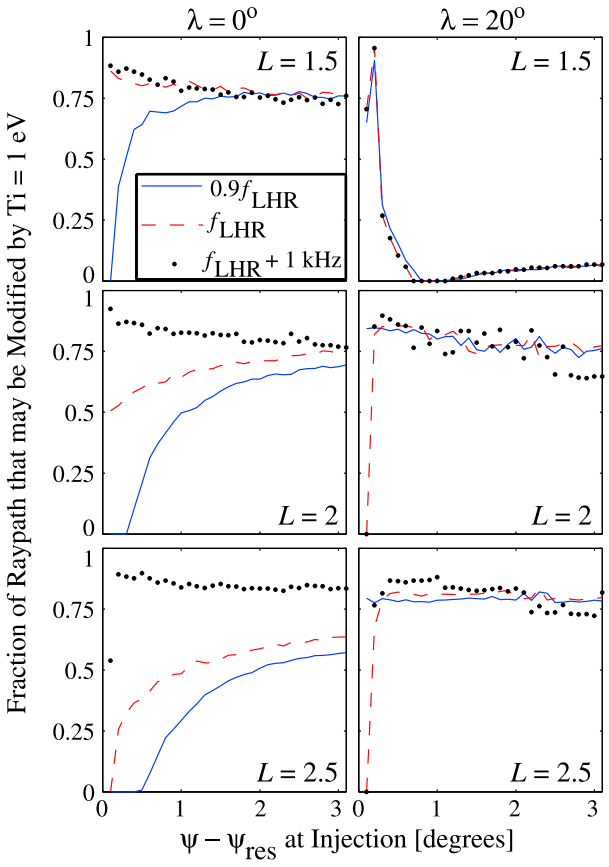

Figure 6. Fraction of time where a finite ion temperature may modify the ray propagation for given injection frequencies and locations. The three *L* shell locations are shown across the rows. (left column) For injection at the equator and (right column) for injection at a latitude of $\lambda = 20°$. The frequency and initial wave normal angles chosen are specified in Table 1.

effects may significantly modify these raypaths. The final outcome may be that four or five sources—instead of the three sources predicted in Paper I—are needed to completely fill the plasmasphere with whistler mode wave energy.

To determine the potential effects of a finite ion temperature on the precipitation signatures shown in Paper II would require knowing how the *k* vector of the wave packet varies along the path. Without this knowledge it is not possible to calculate the effectiveness of the wave-particle interaction and thus determine the energetic electron precipitation. We do argue, however, that the conclusions from Paper II regarding the variation of the *k* vector for wave packets propagating with ψ close to ψ_{res} will remain unchanged even with thermal effects. As discussed in Paper II, in situ injections are limited to frequencies around the lower hybrid resonance and initial injection angles close to 90° (if $f < f_{LHR}$) or to ψ_{res} (for $f > f_{LHR}$). Cold plasma ray tracing also shows that for such injection angles and frequencies, the wave normal angle remains highly oblique either close to 90° (closed refractive index surface) or close to ψ_{res} (open refractive index surface). It can also be inferred that the initial propagation paths of such rays will remain mostly unchanged by thermal effects. We infer this conclusion by examining Figure 5. Note that a 2.3 kHz ($f < f_{LHR}$) wave injected at −89.9° always propagates with its wave frequency significantly below the local f_{LHR}. Accordingly, the refractive index surface is always closed and incorporating thermal effects will not change the propagation or the wave *k* vector along the raypath as was illustrated in Figure 4a. In the other panels of Figure 5, the wave frequency is seen to periodically exceed the local f_{LHR} along the path by a few hundred hertz. As we have shown above, the effect of a finite temperature at these points would be to close a previously open refractive index surface. This would make these wave packets propagate along a trajectory similar to the case where f_{LHR} is never exceeded. So warm plasma ray tracing would make most rays encounter only closed refractive index surfaces, but the net effect would be to keep the wave *k* vector highly oblique, which happens anyway under the cold plasma formulation (see Paper II). So the closing of the refractive index by thermal effects will not affect the wave normal angle significantly, but it may slightly hasten magnetospheric reflections. We therefore predict that the major conclusion of *Kulkarni et al.* [2008]—that few kilohertz magnetospherically reflecting whistlers will precipitate significantly more energetic electrons than a single pass interaction—remains accurate. The specific numerical values, however, must be recalculated to verify these predictions.

4. Conclusion

We have extended previous theoretical work by including ions in the fully adiabatic warm plasma theory [*Sitenko and Stepanov*, 1957; *Buneman*, 1961; *Aubry et al.*, 1970]. We used this methodology to calculate the refractive index surfaces, accounting for a finite electron and hydrogen ion temperature, for few

kilohertz magnetospherically reflecting whistler mode waves. The primary effect of including temperature is to close the refractive index surface for frequencies above the local lower hybrid resonance frequency, f_{LHR}. Based on these results and the analysis from *Kulkarni et al.* [2006, 2008], we conclude that at the frequencies and locations of interest, it is more important to consider a finite ion rather than electron temperature. Specifically, for the purpose of controlled precipitation of radiation belt electrons using in situ sources, a finite ion temperature will more tightly close the refractive index surface. While the propagation of individual raypaths may change with thermal effects, we nonetheless predict that the total region of illumination will not change by more than 0.1*L* from the results in *Kulkarni et al.* [2006]. Fully incorporating warm plasma theory into our calculations may indicate that four or five in situ sources, rather than the three predicted in our previous work, are needed to fill the plasmasphere with whistler mode wave energy.

In addition to changing the propagation characteristics, warm plasma theory may modify our previous precipitation calculations. A warm plasma ray tracer is necessary to determine exactly how these numbers will change. Nevertheless, we are confident that a more detailed analysis will retain the major conclusion from *Kulkarni et al.* [2008]: compared to a single-pass interaction, magnetospherically reflecting whistler mode waves will induce more > 1 MeV electron precipitation.

While the approach used here is an approximation compared to the exact kinetic theory described in the text by *Stix* [1962], *Fang and Andrews* [1971] have noted that the fully adiabatic warm plasma theory yields accurate results. It should be noted that the *Fang and Andrews* [1971] analysis focused on frequencies near the upper hybrid resonance frequency, not few kilohertz whistler mode waves, and their conclusion may change with the frequency range studied. A more recent model developed by *Altman and Suchy* [2004] includes more terms than those used in this work and might better account for thermal effects. Future studies should determine which warm plasma model is best suited for the frequency range of interest and appropriately include it in the ray tracing calculation.

Acknowledgments

The numerical codes used to generate results in this paper are available from the corresponding author (mark.golkowski@ucdenver.edu). This research was supported by ONR MURI award 528828 to the University of Maryland by AFRL award FA9453-11-C-0011 to Stanford University with subaward 27239350-50917-B to CU Denver and NSF CAREER award AGS-1254365 to Mark Gołkowski.

Michael Balikhin thanks Viacheslav Pilipenko and another reviewer for their assistance in evaluating this paper.

References

Abel, B., and R. M. Thorne (1998a), Electron scattering loss in the Earth's inner magnetosphere: 1. Dominant physical processes, *J. Geophys. Res.*, *104*, 2385–2396, doi:10.1029/97JA02919., (Correction, *J. Geophys. Res.*, *104*, 4627, 1999.)

Abel, B., and R. M. Thorne (1998b), Electron scattering loss in the Earth's inner magnetosphere: 2. Sensitivity to model parameters, *J. Geophys. Res.*, *103*, 2397–2408, (Correction, *J. Geophys. Res.*, 104, 4627, 1999.)

Altman, C., and K. Suchy (2004), Wave modes in a magnetoplasma with anisotropic perturbation pressure-fluid and kinetic calculations, *J. Plasma Phys.*, *70*(4), 463–479.

Aubry, M. P., J. Bitoun, and Ph. Graff (1970), Propagation and group velocity in a warm magnetoplasma, *Radio Sci.*, *5*, 635–645.

Bittencourt, J. A. (2004), *Fundamentals of Plasma Physics*, Springer, New York.

Buneman, O. (1961), Gas law and conductivity of a collision-free plasma, *Phys. Fluids*, *4*, 669–680, doi:10.1063/1.1706383.

Carpenter, D. L., and R. R. Anderson (1992), An ISEE/whistler model of equatorial electron-density in the magnetosphere, *J. Geophys. Res.*, *97*(A2), 1097–1108.

Edgar, B. C. (1972), The structure of the magnetosphere as deduced from magnetospherically reflected whistlers, *Tech. Rep. 3438-2*, Radiosc. Lab., Stanford Electron. Lab., Stanford Univ., Stanford, Calif.

Foust, F. R., U. S. Inan, T. F. Bell, and N. G. Lehtinen (2010), Quasi-electrostatic whistler mode wave excitation by linear scattering of EM whistler mode waves from magnetic field-aligned density irregularities, *J. Geophys. Res.*, *115*, A11310, doi:10.1029/2010JA015850.

Graf, K. L., U. S. Inan, and M. Spasojevic (2011), Transmitter-induced modulation of subionospheric VLF signals: Ionospheric heating rather than electron precipitation, *J. Geophys. Res.*, *116*, A12313, doi:10.1029/2011JA016996.

Graf, K. L., N. G. Lehtinen, M. Spasojevic, M. B. Cohen, R. A. Marshall, and U. S. Inan (2013), Analysis of experimentally validated trans-ionospheric attenuation estimates of VLF signals, *J. Geophys. Res. Space Physics*, *118*, 2708–2720, doi:10.1002/jgra.50228.

Fang, M. T. C., and M. K. Andrews (1971), Plasma models of the topside ionosphere and electrostatic wave propagation, *J. Plasma Phys.*, *6*(3), 567–577.

Gołkowski, M., M. B. Cohen, D. L. Carpenter, and U. S. Inan (2011), On the occurrence of ground observations of ELF/VLF magnetospheric amplification induced by the HAARP facility, *J. Geophys. Res.*, *116*, A04208, doi:10.1029/2010JA016261.

Haselgrove, J. (1954), Ray theory and a new method for ray tracing, pp. 355–364, Cambridge, England.

Hashimoto, K., I. Kimura, and H. Kumagai (1977), Estimation of electron temperature by VLF waves propagating in directions near the resonance cone, *Planet. Space Sci.*, *25*, 871–877.

Helliwell, R. A. (1965), *Whistlers and Related Ionospheric Phenomena*, Stanford Univ. Press, Stanford, Calif.

Hines, C. O. (1957), Heavy-ion effects in audio frequency radio propagation, *J. Atmos. Terr. Phys.*, *11*(1), 36–42.

Inan, U. S. (1987), Gyroresonant pitch angle scattering by coherent and incoherent whistler mode waves in the magnetosphere, *J. Geophys. Res.*, *92*, 127–142.

Inan, U. S., and T. F. Bell (1977), The plasmapause as a VLF waveguide, *J. Geophys. Res.*, *82*, 2819–2827, doi:10.1029/JA082i019p02819.

Inan, U. S., T. F. Bell, J. Bortnik, and J. M. Albert (2003), Controlled precipitation of radiation belt electrons, *J. Geophys. Res.*, *108*(A5), 1186, doi:10.1029/2002JA009580.

Inan, U. S., M. Golkowski, M. K. Casey, R. C. Moore, W. Peter, P. Kulkarni, P. Kossey, E. Kennedy, S. Meth, and P. Smit (2007), Subionospheric VLF observations of transmitter-induced precipitation of inner radiation belt electrons, *Geophys. Res. Lett.*, *34*, L02106, doi:10.1029/2006GL028494.

Kennel, C. F., and H. E. Petschek (1966), Limit on stably trapped particle fluxes, *J. Geophys. Res.*, *71*, 1–28.

Kimura, I. (1966), Effects of ions on whistler-mode ray tracing, *Radio Sci.*, *1*(3), 269–283.

Kulkarni, P., U. S. Inan, and T. F. Bell (2006), Whistler mode illumination of the plasmaspheric resonant cavity via in situ injection of ELF/VLF waves, *J. Geophys. Res.*, *111*, A10215, doi:10.1029/2006JA011654.

Kulkarni, P., U. S. Inan, and T. F. Bell (2008), Energetic electron precipitation induced by space based VLF transmitters, *J. Geophys. Res.*, *113*, A09203, doi:10.1029/2008JA013120.

Lyons, L. R., R. M. Thorne, and C. F. Kennel (1972), Pitch angle diffusion of radiation belt electrons within the plasmasphere, *J. Geophys. Res.*, *77*, 3455.

Mann, G., P. Hackenberg, and E. Marsch (1997), Linear mode analysis in multi-ion plasmas, *J. Plasma Phys.*, *58*(2), 205–221.

Poeverlein, H. (1948), Strahlwege von Radiowellen in der ionosphaäre, *Sitz. Bayerischen Akad. Wiss.*, *1*, 175–201.

Sazhin, S. S. (1985), Almost parallel electromagnetic wave propagation in a hot anisotropic plasma, *J. Atmos. Terr. Phys.*, *47*(6), 517–522.

Sazhin, S. S. (1986), Quasi-electrostatic wave propagation in a hot anisotropic plasma, *Planet. Space Sci.*, *34*(6), 497–509.

Sazhin, S. S., and E. M. Sazhina (1985), Quasielectrostatic whistler-mode propagation, *Planet. Space Sci.*, *33*(3), 295–303.

Shao, X., B. Eliasson, A. S. Sharma, G. Milikh, and K. Papadopoulos (2012), Attenuation of whistler waves through conversion to lower hybrid waves in the low-altitude ionosphere, *J. Geophys. Res.*, *117*, A04311, doi:10.1029/2011JA017339.

Sitenko, A. G., and K. N. Stepanov (1957), On the oscillations of an electron plasma in a magnetic field, *Soviet Physics JETP*, *4*(4), 512–520.

Starks, M. J., R. A. Quinn, G. P. Ginet, J. M. Albert, G. S. Sales, B. W. Reinisch, and P. Song (2008), Illumination of the plasmasphere by terrestrial very low frequency transmitters: Model validation, *J. Geophys. Res.*, *113*, A09320, doi:10.1029/2008JA013112.

Stix, H. (1962), *The Theory of Plasma Waves*, McGraw-Hill, New York.

Tao, X., J. Bortnik, and M. Friedrich (2010), Variance of transionospheric VLF wave power absorption, *J. Geophys. Res.*, *115*, A07303, doi:10.1029/2009JA015115.

Wang, T. N. C., and T. F. Bell (1969), Radiation resistance of a short dipole immersed in a cold magnetoionic medium, *Radio Sci.*, *4*(2), 167–177.